Vol 15 No 10, October 2006
1009-1963/2006/15(10)/2306-09

Chinese Physics

© 2006 Chin. Phys. Soc.
and IOP Publishing Ltd

Soliton-like pulse timing jitter in dispersion-managed systems

Li Qi-Liang(李齐良)[a)b)†], Li Qing-Shan(李庆山)[a)], and Lin Li-Bin(林理彬)[b)]

[a)] *School of Communication, Hangzhou Dianzi University, Hangzhou* 310018, *China*

[b)] *Institute of Physics, Sichuan University, Chengdu* 610064, *China*

(Received 7 April 2006; revised manuscript received 26 April 2006)

In this paper, the timing jitter in dispersion-managed soliton-like systems with the Gaussian pulse is studied by using two methods. Firstly, the derivation of the dynamic equations for the evolution of soliton-like parameters and the timing jitter expressions for the dispersion-managed soliton-like systems are carried out by the perturbed variational method. By analysing and simulating these timing jitter expressions, one can find that the timing jitter is induced by the amplified spontaneous emission noise and the frequency shift, etc. Nonlinear gain can suppress the timing jitter. The chirp sign and the filters action have also effects on the total timing jitter. Secondly, the timing jitter is calculated and analysed by using the moment method. The results of the two methods prove to be consistent with each other.

Keywords: timing jitter, variational analysis, dispersion-managed soliton

PACC: 4225B, 4281D

1. Introduction

The idea of periodic dispersion management is quite simple. It involves mixing fibres with positive and negative group velocity dispersions in a periodic fashion so that the total dispersion over each period is close to zero. If the average dispersion of each map period is nearly zero, the dispersion can be compensated over each map period.[1] Optical solitons may soon be the primary carriers for long- and short-distance information transmission because, unlike pulses in a linear dispersive fibre, solitons are self-confined, propagating over a long distance without changing their shape. So solitons are being studied widely.[2−6] Dispersion-managed soliton (DMS) has been attracting considerable interest recently in optical communication systems because of their superb characteristics which are not observed in conventional solitons.[7,8] In particular, sufficiently strong periodic dispersion management allows for stationary propagation of nonlinear return-to-zero pulses with finite energy when the average dispersion is close or even equal to zero. This helps suppress the Gordon–Haus effect without sacrificing the signal-to-noise ratio (SNR). Furthermore, the amplitude of DMS can be made sufficiently large to maintain sufficiently large SNR by a proper choice of the magnitude of the dispersion map. That is, a DMS can be very robust in periodically amplified all-optical transmission systems.[9]

Optical signal transmission in long-haul optical communication systems is limited by amplified spontaneous emission (ASE) added to optical amplifiers needed for compensation of fibre losses. The ASE induces frequency shifts that accumulate and introduce timing jitter in the presence of group velocity dispersion (GVD) as the signal propagates along the fibre.[10] The time variance was calculated for the first time by Gordon and Haus for a hyperbolic secant soliton pulse propagating in a fibre with uniform dispersion.[11,12] They drew a conclusion that the timing fluctuations along the transmission line grow as the cube of propagation distance.[13] However, one cannot directly apply the Gordon–Haus theory in most cases because the pulse shapes in DMS systems differ significantly from the hyperbolic-secant shape. For DMS, the pulse shapes range from hyperbolic-secant to Gaussian to flattop, depending on the strength of the dispersion management.[14−16] In the former research, Gordon–Haus timing jitter in dispersion-managed systems was calculated using the moment method.[17−19]

In this paper, the timing jitter in the DMS system with filters and amplifiers is studied by using the perturbed variational method. This paper is organized as follows. In Section 2 the perturbed nonlinear Schrödinger equation (NLSE) and the noise correla-

†E-mail: liqiliang2@yahoo.com.cn

tion properties are introduced. In Section 3 the timing jitter of the DMS system is calculated and analysed. Firstly, we derive the dynamic equations for the evolution of soliton-like parameters and timing jitter expressions in the presence of the quadratic nonlinear gain, filter and ASE action, and analyse various factors of induced timing jitter. Secondly, we simulate the DMS system with the positive and negative chirps, obtain the figures of the timing jitter versus transmission distance, and analyse these figures. Thirdly, in order to validate the timing jitter calculated by the perturbed variational method, we recount the timing jitter by using the moment method, and compare the results obtained by the two methods. Finally, in Section 4 the main results of this paper are summarized.

2. Basic theory

In dispersion-managed schemes, optical pulse propagation can be governed by the following perturbed NLSE:[13,20]

$$\mathrm{i}\frac{\partial u}{\partial z}+\frac{1}{2}\beta_2\frac{\partial^2 u}{\partial t^2}+\gamma|u|^2u=\mathrm{i}\varepsilon R, \tag{1}$$

where $u(z,t)$ is the slowly varying envelope of electric field, z is the propagation distance and t is the retarded time. β_2 is the GVD coefficient and can be written as

$$\beta_2=\begin{cases}\beta_{21}, & 0<z<L_1,\\ \beta_{22}, & L_1<z<L_{\mathrm{map}},\end{cases}$$

where $L_{\mathrm{map}}=L_1+L_2$, L_{map} is the dispersion-managed period and $\beta_{2\mathrm{j}}$ is the GVD parameter for the fibre segment of length $L_j(j=1,2);\gamma=2\pi n_2/\lambda A_{\mathrm{eff}}$. is the Kerr nonlinearity coefficient, where n_2 is the nonlinear refractive index and A_{eff} is the fibre's effective area. For a strong dispersion management, path average dispersion coefficient $\langle\beta_2\rangle$ approximates to zero, namely

$$\langle\beta_2\rangle=(\beta_{21}L_1+\beta_{22}L_2)/L_{\mathrm{map}}\approx 0. \tag{2}$$

By considering the combined action of excess gain, quadratic nonlinear gain, filters and ASE, perturbation εR has the following form

$$\varepsilon R=\frac{1}{2}(\alpha+2\kappa|u|^2+\eta\frac{\partial^2}{\partial t^2})u+\chi(z,t), \tag{3}$$

where α is the excess gain or loss coefficient, κ is the quadratic nonlinear gain or loss (which describes, for instance, fast saturable absorption, 2-photon absorption if negative), $\eta=2\ln 2/(B_{\mathrm{f}}^2 z_{\mathrm{f}})$ represents the filter strength parameter, B_{f} is the filter's band width and z_{f} is the filtering period.[21] ASE is accounted for as the additive white Gaussian noise (AWGN) term $\chi(z,t)$, with the following correlation properties:

$$\langle\chi(z,t)\rangle=\langle\chi(z,t)\chi(z',t')\rangle=0, \tag{4}$$

$$\langle\chi(z,t)\chi^*(z',t')\rangle=2g_0\hbar\omega_0 n_{\mathrm{sp}}(z)\delta(z-z')\delta(t-t'), \tag{5}$$

where g_0 is the amplification coefficient inside the amplifier, $\hbar\omega_0$ is the photon energy at the signal frequency, and n_{sp} is the spontaneous emission factor.

Assuming that a chirped Gaussian pulse is launched initially and maintains the Gaussian form during propagation, the optical field at any point along the fibre can be written as

$$u=A\exp\left\{-\frac{(t-T)^2}{2\tau^2}+\mathrm{i}\left[\omega(t-T)+c(t-T)^2+\theta\right]\right\}, \tag{6}$$

where A, T, $2\sqrt{\ln 2}\tau$, $\omega/2\pi$, $c/4\pi$, and θ represent the pulse's amplitude, temporal position, width (FWHM), frequency, chirp and phase, respectively.

3. Calculation and discussion on timing jitter

3.1. Calculation and analysis by the perturbed variational method

Now we study the timing jitter of the DMS systems using the perturbed variational method. The unperturbed Lagrangian density of Eq.(1) has the following form

$$L' = \frac{\mathrm{i}}{2}\left(u^*\frac{\partial u}{\partial z} - u\frac{\partial u^*}{\partial z}\right) - \frac{\beta_2}{2}\left|\frac{\partial u}{\partial t}\right|^2 + \frac{\gamma}{2}|u|^4. \quad (7)$$

The averaged Lagrangian density L is defined as

$$L = \int_{-\infty}^{+\infty} L'\mathrm{d}t. \quad (8)$$

Since one sees εR as the perturbation and it is independent of u^*, the perturbed variational equation can be written as[22,23]

$$\frac{\mathrm{d}}{\mathrm{d}z}\left(\frac{\partial L}{\partial \dot{X}_j}\right) - \frac{\partial L}{\partial X_j} = 2\mathrm{Re}\int_{-\infty}^{+\infty}\varepsilon R\frac{\partial u^*}{\partial X_j}\mathrm{d}t, \quad (9)$$

where X_j can represent $A, T, \tau, \omega, c, \theta$ separately and $\dot{X}_j$ represents $\partial X_j/\partial z$. Substituting Eq.(6) into (7), integrating the Lagrangian density L' in Eq.(7) over t from $-\infty$ to $+\infty$, we can find the averaged Lagrangian density L

$$\begin{aligned} L = {} & \sqrt{\pi}\omega\tau A^2\frac{\mathrm{d}T}{\mathrm{d}z} - \frac{\sqrt{\pi}}{2}A^2\tau^3\frac{\mathrm{d}c}{\mathrm{d}z} - \sqrt{\pi}A^2\tau\frac{\mathrm{d}\theta}{\mathrm{d}z} \\ & -\frac{\sqrt{\pi}}{4\tau}\beta_2 A^2 - \frac{\sqrt{\pi}}{2}\beta_2\omega^2A^2\tau \\ & -\sqrt{\pi}\beta_2A^2c^2\tau^3 + \frac{\sqrt{2\pi}}{4}\gamma A^4\tau. \end{aligned} \quad (10)$$

We also can obtain the dynamic equations by use of Eqs.(9) and (10)

$$\frac{\mathrm{d}T}{\mathrm{d}z} = (\beta_2-\eta)\omega + \frac{2}{E}\mathrm{Re}\int_{-\infty}^{+\infty}[-\mathrm{i}\chi u^*(t-T)]\mathrm{d}t, \quad (11a)$$

$$\frac{\mathrm{d}\omega}{\mathrm{d}z} = \frac{2}{E}\mathrm{Re}\int_{-\infty}^{+\infty}\left\{-\chi u^*\left[\frac{t-T}{\tau^2} + \mathrm{i}2c(t-T)\right]\right\}\mathrm{d}t, \quad (11b)$$

$$\frac{\mathrm{d}\tau}{\mathrm{d}z} = 2(\beta_2-\eta)c\tau + \frac{1}{E}\left\{2\mathrm{Re}\int_{-\infty}^{+\infty}\left[-\mathrm{i}\chi u^*\frac{(t-T)^2}{\tau}\right]\mathrm{d}t - \tau\mathrm{Re}\int_{-\infty}^{+\infty}(-\mathrm{i}\chi u^*)\mathrm{d}t\right\}, \quad (11c)$$

$$\frac{\mathrm{d}A}{\mathrm{d}z} = -(\beta_2-\eta)Ac + \frac{\alpha A}{2} + \frac{A}{2E}\left\{3\mathrm{Re}\int_{-\infty}^{+\infty}(-\mathrm{i}\chi u^*)\mathrm{d}t - 2\mathrm{Re}\int_{-\infty}^{+\infty}\left[-\mathrm{i}\chi u^*\frac{(t-T)^2}{\tau^2}\right]\mathrm{d}t\right\}, \quad (11d)$$

$$\frac{\mathrm{d}c}{\mathrm{d}z} = \frac{(\beta_2-\eta)(1-4\tau^4c^2)}{2\tau^4} - \frac{\sqrt{2}A(\gamma-\kappa)}{4\tau^2} + \frac{1}{E}\left\{\mathrm{Re}\int_{-\infty}^{+\infty}\chi u^*\left[\frac{1}{\tau^2} - \frac{(t-T)^2}{\tau^4}\right]\mathrm{d}t\right\}, \quad (11e)$$

$$\begin{aligned} \frac{\mathrm{d}\theta}{\mathrm{d}z} = {} & \frac{1}{2\tau^2}(\beta_2-\eta)(\omega^2\tau^2-1) + \frac{5\sqrt{2}}{8}A^2(\gamma-\kappa) - \frac{\alpha}{2} \\ & + \frac{1}{2E}\left\{4\omega\mathrm{Re}\int_{-\infty}^{+\infty}\Big[-\mathrm{i}\chi u^*(t-T)\Big]\mathrm{d}t - 3\mathrm{Re}\int_{-\infty}^{+\infty}\chi u^*\mathrm{d}t + 2\mathrm{Re}\int_{-\infty}^{+\infty}\chi u^*\frac{(t-T)^2}{\tau^2}\mathrm{d}t\right\}, \end{aligned} \quad (11f)$$

where $E = \int_{-\infty}^{+\infty}|u|^2\mathrm{d}t$ is the energy of the pulse.

The fundamental parameter determining the timing jitter is the variance of the temporal position T. So we choose the dynamic equations related to T and change them slightly:

$$\frac{\mathrm{d}T}{\mathrm{d}z} = (\beta_2-\eta)\omega + \frac{\mathrm{i}}{E}\int_{-\infty}^{+\infty}(t-T)(\chi^*u - \chi u^*)\mathrm{d}t, \quad (12a)$$

$$\frac{\mathrm{d}\omega}{\mathrm{d}z} = -\frac{1}{E}\int_{-\infty}^{+\infty}\frac{t-T}{\tau^2}(\chi^*u + \chi u^*)\mathrm{d}t + \frac{\mathrm{i}}{E}\int_{-\infty}^{+\infty}2c(t-T)(\chi^*u - \chi u^*)\mathrm{d}t. \quad (12b)$$

From Eq.(12b), one can see that the frequency shift is induced by the ASE noise and is related to the time offset and the pulse chirp. The frequency ω will not change without the noise terms. The time shift comes from the common action of the GVD and the frequency shift, which can be seen from Eq.(12a). The term $(\beta_2-\eta)\omega$ represents a contribution to the timing jitter, and is produced by the GVD, the filter action and the frequency. From this term, one can see that the filter action may suppress the increase of the timing jitter. Neglecting the impact of the noise terms, the temporal position T will breathe periodically. In Eqs.(12), the noise terms are approximate due to the stochastic characteristic of the ASE noise, whereas the term $(\beta_2-\eta)\omega$ is exact.

Now we evaluate the variances and cross correlation of the noise terms in Eqs.(12) using Eqs.(4)–(6). For simplicity, we define the following variations

$$\delta T = \frac{\mathrm{i}}{E}\int_{-\infty}^{+\infty}(t-T)(\chi^* u-\chi u^*)\mathrm{d}t, \tag{13a}$$

$$\delta\omega = -\frac{1}{E}\int_{-\infty}^{+\infty}\frac{t-T}{\tau^2}(\chi^* u+\chi u^*)\mathrm{d}t+\frac{\mathrm{i}}{E}\int_{-\infty}^{+\infty}2c(t-T)(\chi^* u-\chi u^*)\mathrm{d}t, \tag{13b}$$

where δT and $\delta\omega$ represent the random time and frequency shifts due to the ASE noise. It is not difficult to find that

$$\langle\delta T^2\rangle = \frac{2S}{E^2}\int_{-\infty}^{+\infty}(t-T)^2|u|^2\mathrm{d}t = \frac{S\tau^2}{E}, \tag{14}$$

$$\langle\delta\omega^2\rangle = \frac{2S}{E^2}\int_{-\infty}^{+\infty}\frac{(t-T)^2}{\tau^4}|u|^2\mathrm{d}t+\frac{2S}{E^2}\int_{-\infty}^{+\infty}4c^2(t-T)^2|u|^2\mathrm{d}t = \frac{S(1+4c^2\tau^2)}{E\tau^2}, \tag{15}$$

$$\langle\delta T\delta\omega\rangle = \frac{4Sc}{E^2}\int_{-\infty}^{+\infty}(t-T)^2|u|^2\mathrm{d}t = \frac{2Sc\tau^2}{E}, \tag{16}$$

where $S=2g_0\hbar\omega_0 n_{\mathrm{sp}}$. Solutions of Eqs.(12) are

$$T = T_1+T_2, \tag{17}$$

where

$$\begin{aligned}
T_1 &= \int_0^z(\beta_2-\eta)\omega\mathrm{d}z',\\
T_2 &= \frac{\mathrm{i}}{E}\int_0^z\left[\int_{-\infty}^{+\infty}(t-T)(\chi^* u-\chi u^*)\mathrm{d}t\right]\mathrm{d}z',\\
\omega &= -\frac{1}{E}\int_0^z\left[\int_{-\infty}^{+\infty}\frac{(t-T)}{\tau^2}(\chi^* u+\chi u^*)\mathrm{d}t\right]\mathrm{d}z'+\frac{\mathrm{i}}{E}\int_0^z\left[\int_{-\infty}^{+\infty}2c(t-T)(\chi^* u-\chi u^*)\mathrm{d}t\right]\mathrm{d}z'.
\end{aligned} \tag{18}$$

As is seen from Eq.(17), the temporal position T is a superposition of the time shift T_1 induced by the frequency shift and the time shift T_2 due to the direct impact of the noise on the pulse. Using Eqs.(5), (17) and (18), we can calculate the variance of the

temporal position T,

$$\sigma_T^2 = \langle T^2\rangle - \langle T\rangle^2 = \langle T_1^2\rangle + 2\langle T_1T_2\rangle + \langle T_2^2\rangle. \quad (19)$$

In order to make calculation compact and explicit, we define the following components:

$$\begin{aligned} \delta q_1 &= 2\mathrm{i}\sqrt{g\hbar\omega_0 n_{\mathrm{sp}}}(t-T)u/E, \\ \delta q_2 &= -2\sqrt{g\hbar\omega_0 n_{\mathrm{sp}}}(t-T)u/E\tau^2, \\ \delta q_3 &= 4\mathrm{i}\sqrt{g\hbar\omega_0 n_{\mathrm{sp}}}(t-T)cu/E. \end{aligned} \quad (20)$$

We find that

$$\begin{aligned} \langle T_1^2\rangle &= \int_0^z [\beta_2(z_1)-\eta(z_1)]\,\mathrm{d}z_1 \int_0^{z_1} [\beta_2(z_2)-\eta(z_2)]\,\mathrm{d}z_2 \cdot \int_0^{z_2} \left[\int_{-\infty}^{+\infty} (\delta q_2\delta q_2^* + \delta q_3\delta q_3^*)\mathrm{d}t\right]\mathrm{d}z', \\ 2\langle T_1T_2\rangle &= \int_0^z [\beta_2(z_1)-\eta(z_1)]\,\mathrm{d}z_1 \int_0^{z1} \left(\int_{-\infty}^{+\infty} \delta q_1\delta q_3^*\mathrm{d}t\right)\mathrm{d}z', \\ \langle T_2^2\rangle &= \int_0^z \left(\int_{-\infty}^{+\infty} \delta q_1\delta q_1^*\mathrm{d}t\right)\mathrm{d}z'. \end{aligned} \quad (21)$$

In Eqs.(21), $\langle T_1^2\rangle$ represents the timing jitter induced by the frequency shift alone, $\langle T_2^2\rangle$ represents the timing jitter induced by the time offset alone, and $2\langle T_1T_2\rangle$ represents the interference between the two effects, which can either increase or decrease the total timing jitter depending on the sign of the c, due to

$$\int_{-\infty}^{+\infty} \delta q_1\delta q_3^*\mathrm{d}t = \frac{8g\hbar\omega_0 n_{\mathrm{sp}}c}{E^2}\int_{-\infty}^{+\infty}(t-T)^2|u|^2\mathrm{d}t = \frac{4\sqrt{\pi}g\hbar\omega_0 n_{\mathrm{sp}}cA^2\tau^3}{E^2}. \quad (22)$$

When $(\beta_2-\eta)c$ is positive, the timing jitter increases; otherwise the timing jitter decreases. From these descriptions, one can find that the timing jitter of the DMS system is induced by the frequency shift, the time offset and the interference between the two effects. Moreover, the chirp sign and the filter action have also effects on the total timing jitter.

3.2. Analysis of the timing jitter in the DMS system

To study the timing jitter of a chirped DMS system with a Gaussian pulse, we consider a 40Gbit/s soliton-like system with a dispersion map consisting of 50 km of anomalous-GVD fibre ($\beta_{\mathrm{a}} = -3.75\mathrm{ps}^2/\mathrm{km}$) and 50 km of normal-GVD ($\beta_n = 3.73\mathrm{ps}^2/\mathrm{km}$), $\langle\beta_2\rangle = -0.01\mathrm{ps}^2/\mathrm{km}$. The parameters for the input Gaussian pulse have values $\tau_0 = 3\mathrm{ps}$, $c_0 = 0.03\mathrm{ps}^{-2}$, $E_0 = 0.13\mathrm{pJ}$. Other parameters' values are as follows: Amplifier spontaneous emission factor $n_{\mathrm{sp}} = 1.5$, the strength of filter $\eta = 0.04\mathrm{ps}^2/\mathrm{km}$, the central wavelength of optical wave $\lambda = 1.55\mu\mathrm{m}$, thus the photon energy $\hbar\omega_0 = 1.283\times10^{-7}\mathrm{pJ}$, the periods of the lumped amplifiers are 100km, the Kerr nonlinearity coefficient $\gamma = 1.7\mathrm{W}^{-1}/\mathrm{km}$, and the quadratic nonlinear gain $\kappa = 0.17\mathrm{W}^{-1}/\mathrm{km}$.

We obtain the timing jitter versus distance z for the positive chirped DMS system using Eqs.(19)–(21), and we also show the individual contributions of $\langle T_1^2\rangle$, $2\langle T_1T_2\rangle$ and $\langle T_2^2\rangle$ in Fig.1. One can see in Fig.1 that the curves take on indentations, which result from the compensation of anomalous dispersion fibres. Without the dispersion compensation the timing jitter will be very serious, and then cause the SNR to decrease. So the compensation improves the transmission performance of the system. From Fig.1 and Eqs.(21) one

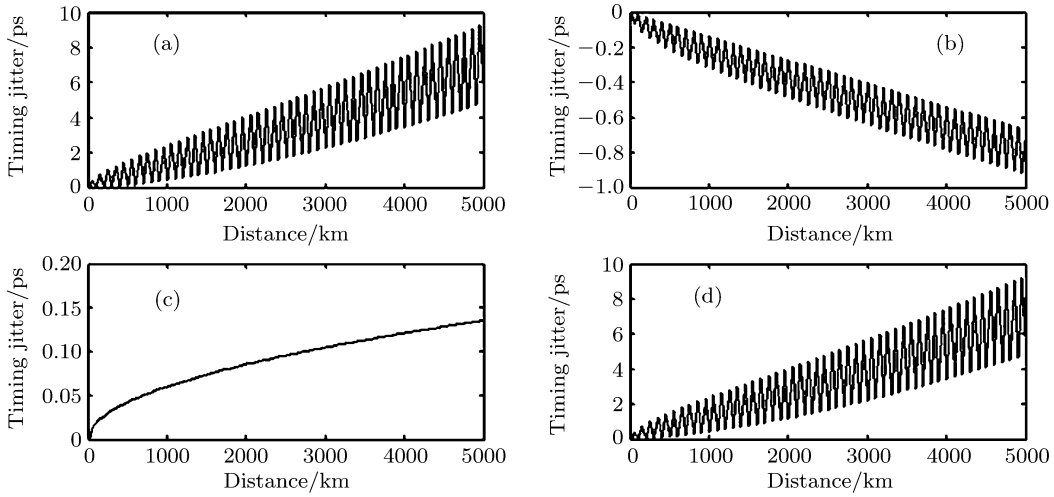


Fig.1. Timing jitter versus distance z for a positive chirped dispersion-managed soliton-like system. In (a), (b) and (c) are shown the individual contributions of the $\langle T_1^2 \rangle$, $2\langle T_1 T_2 \rangle$ and $\langle T_2^2 \rangle$ to timing jitter, (d)shows the total timing jitter versus distance z.

can find that $\langle T_1^2 \rangle$ and $\langle T_2^2 \rangle$ are always positive. However, for the positive chirp, $2\langle T_1 T_2 \rangle$ is negative, which means that the positive chirp can suppress the timing jitter caused by the frequency shift and time offset. On the contrary, if we only change the sign of the c, we can simulate the timing jitter versus distance z for the negative-chirped DMS system in Fig.2. As $2\langle T_1 T_2 \rangle$ is positive, the total timing jitter increases. Hence, the chirp sign has effect on the total timing jitter.

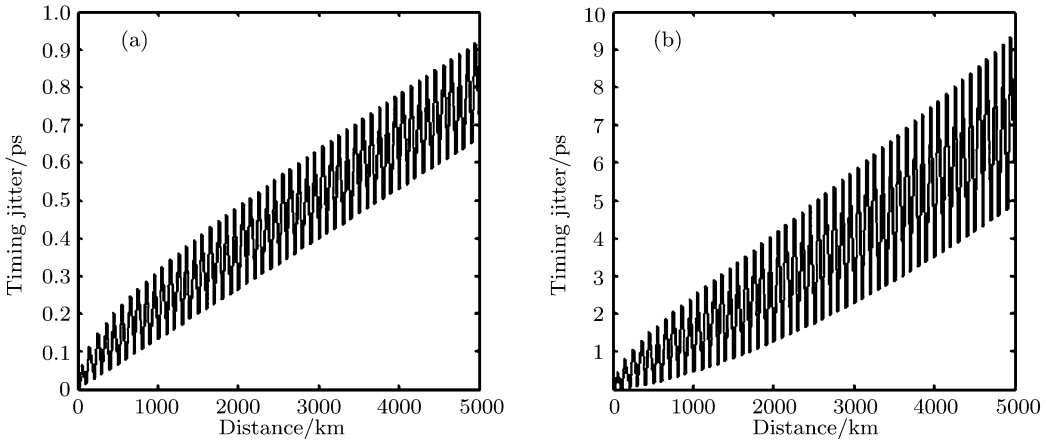


Fig.2. Timing jitter versus distance z for a negative-chirped dispersion-managed soliton-like system. (a) shows the individual contribution of the $2\langle T_1 T_2 \rangle$ to timing jitter, (b)shows the total timing jitter versus distance z.

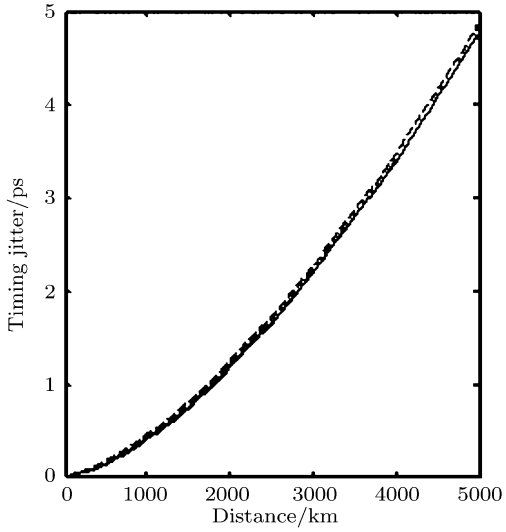


Fig.3. Timing jitter versus distance z for a positive- and negative-chirped dispersion-managed soliton-like system. Solid curve is for the case of the positive chirp, dashed curve is for the case of the negative chirp.

Figure 3 shows the timing jitter versus distance z for the positive- and negative-chirped DMS systems. This figure explicitly presents the effect of the chirp on the total timing jitter. After soliton-like pulses are transmitted for 5000km, the timing jitter of the DMS system is 4.89 ps in the case of the negative chirp; however, the timing jitter of the DMS system is 4.80 ps in the case of the positive chirp. Thus, the timing jitter reduces by 0.09 ps, which numerically reflects the effect of the chirp sign on the total timing jitter.

3.3. Derivation of the timing jitter by using the moment method

In order to validate the derivation of the timing jitter using the perturbed variational method, we recount the timing jitter using the moment method, and carry out the simulation. In the moment method, we define the temporal position T' and the frequency ω' as:[17]

$$T' = \frac{1}{E}\int_{-\infty}^{+\infty} t|u|^2 \mathrm{d}t, \tag{23a}$$

$$\omega' = \frac{\mathrm{i}}{2E}\int_{-\infty}^{+\infty} (u^* u_t - u u_t^*)\mathrm{d}t, \tag{23b}$$

where u_t stands for the time derivation. Using Eq.(1), we can find the following dynamic equations for the temporal position T' and the frequency ω'

$$\frac{\mathrm{d}T'}{\mathrm{d}z} = (\beta_2 - \eta)\omega' + \sum_{j=1}^{N} \delta T_j' \delta(z - z_j), \tag{24a}$$

$$\frac{\mathrm{d}\omega'}{\mathrm{d}z} = \sum_{j=1}^{N} \delta\omega_j' \delta(z - z_j), \tag{24b}$$

where $\delta T_j'$ and $\beta\omega_j'$ are the time and frequency shifts imposed on the pulse at the jth amplifier and N is the total number of amplifiers used within the DMS system. Comparing Eqs.(24) with Eqs.(12) which are derived by the perturbed variational method, we find that the exact terms in Eqs.(24a) are the same as those in Eqs.(12a) and the approximate terms all result from the ASE noise. Although the expressions obtained using the two methods are different apparently, the real physics contents are alike.

The variances and cross correlation of $\delta T_j'$ and $\delta\omega_j'$ can be obtained by substituting Eq.(6) into the general formulas derived in Ref.[16]. After some algebra, we obtain

$$\langle \delta T'^2 \rangle = \frac{2S'}{E^2}\int_{-\infty}^{+\infty} (t - T')^2 |B|^2 \mathrm{d}t = \frac{S'\tau^2}{E}, \tag{25}$$

$$\langle \delta\omega'^2 \rangle = \frac{2S'}{E^2}\int_{-\infty}^{+\infty} |B_t|^2 \mathrm{d}t = \frac{S'(1 + 4c^2\tau^2)}{E\tau^2}, \tag{26}$$

$$\langle \delta T' \delta\omega' \rangle = \frac{\mathrm{i}S'}{2E^2}\int_{-\infty}^{+\infty} (t - T')(B^* B_t - B B_t^*)\mathrm{d}t = \frac{2S'c\tau^2}{E}, \tag{27}$$

where $B = u\exp(\mathrm{i}\omega t)$, $S' = n_{\mathrm{sp}}\hbar\omega_0(G-1)$, and G is the gain of each amplifier. Comparing Eqs.(25)–(27) with Eqs.(14)–(16), we can find that the variances and cross correlation of the timing and frequency shifts for the two methods have the same expressions basically.

Now we consider the DMS system with N amplifiers, and calculate the timing jitter σ_t using Eqs.(20)–(23).

$$\sigma_t^2 = \langle T'^2 \rangle - \langle T' \rangle^2 = (S'/E)\tau_0^2[N(1 + 4c^2\tau_0^2) + 2N(N-1)c\tau_0^2 d + 1/6N(N-1)(2N-1)d^2], \tag{28}$$

where $d = \tau_0^{-2}\int_0^{L_A}(\beta_2 - \eta)\mathrm{d}z$, L_A is the amplifier spacing. From Eq.(28), we can also find the effect of the chirp sign on the total timing jitter. When cd is positive, namely, $c(\beta_2-\eta)$ is positive, the timing jitter increases; otherwise the timing jitter decreases. This result is consistent with the above result obtained by the first method.

From the simulation of the timing jitter for the positive-chirped DMS system, we obtain the timing jitter versus distance z obtained using the perturbed variational method and the moment method in Fig.4,

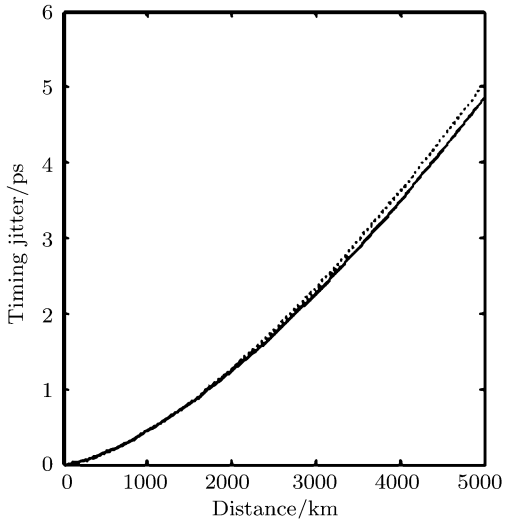


Fig.4. Timing jitter versus distance z obtained using two methods for a positive-chirped dispersion-managed soliton-like system. Solid curve is for the case using the perturbed variational method, doted curve is for the case obtained using the moment method.

respectively. The figure shows that the timing jitter obtained by the perturbed variational method is 4.80ps and that by the moment method is 5.09ps after soliton-like pulses are transmitted through 5000km. The difference between the two results is very small. Hence, it is feasible to analyse the timing jitter for DMS systems by using the perturbed variational method.

4. Conclusions

We have studied the timing jitter for the Gaussian-chirped DMS system, and considered the effects of quadratic nonlinear gain, filters and ASE action on the timing jitter. In Refs.[17]–[20] the chirp sign and nonlinear gain were not considered. However, in the present paper we have considered the effect of them on the timing jitter: the positive chirp decreases the timing jitter; the negative chirp increases it, and nonlinear gain can suppress the timing jitter of DMS. The expressions and figures obtained by the first method show that the timing jitter is induced by the frequency shift and the ASE noise. Moreover, filter action makes the timing jitter grow slowly. So we can suppress the increase of the timing jitter by filters. By analysing the timing jitter expressions calculated by the two methods, we can find that the chirp sign has the same effect on the total timing jitter. Furthermore, the simulations of the timing jitter show that the two methods are consistent with each other. Comparing with Ref.[16], in which the timing jitter is calculated by using the moment method, we have also calculated and analysed the timing jitter using the perturbed variational method. Moreover, we also have taken into consideration the quadratic nonlinear gain action and the effect of the chirp sign on the timing jitter.

References

[1] Agrawal G P 2002 *Fiber-Optic Communication Systems* (New York: Wiley)

[2] Mollenauer L F, Stolen R H and Gordon J P 1980 *Phys. Rev. Lett.* **45** 1095

[3] Li H, Wang T J, Huang D X and Wang D N 2004 *Chin. Phys.* **13** 1447

[4] Chen X W, Lin X S and Lan S 2005 *Chin. Phys.* **14** 366

[5] Cao J N and Guo Q 2005 *Acta Phys. Sin.* **54** 3688 (in Chinese)

[6] Wang Y L, Zhou Z X, Yuan C X, Jiang X Q and Qin R H 2006 *Chin. Phys.* **15** 156

[7] Hirooka T 2000 *Opt. Fiber Technol.* **6** 109

[8] Li H, Wang T J and Huang D X 2004 *Chin. Phys.* **13** 1033

[9] Hasegawa A 2000 *IEEE J. Sel. Top. Quantum Electron* **6** 1161

[10] Santhanam J and Agrawal G P 2003 *J. Opt. Soc. Am.* B **20** 284

[11] Gordon J P and Haus H A 1986 *Opt. Lett.* **11** 665

[12] Haus H A 1991 *J. Opt. Soc. Am.* B **8** 1122

[13] Derevyanko S A, Turitsyn S K and Yakushev D A 2005 *J. Opt. Soc. Am.* B **22** 743

[14] Smith N J, Forysiak W and Doran N J 1996 *Electron. Lett.* **32** 2085

[15] Carter G M, Jacob J M, Menyuk C. R. Golovchenko E A and Pilipetskii A N 1997 *Opt. Lett.* **22** 513

[16] Grigoryan V S, Menyuk C R and Mu R M 1999 *J. Lightwave Technol.* **17** 1347

[17] Santhanam J, McKinstrie C J, Lakoba T I and Agrawal G P 2001 *Opt. Lett.* **26** 1131

[18] McKinstrie C J, Santhanam J and Agrawal G P 2002 *J. Opt. Soc. Am.* B **19** 640
Poutrina Ekaterina and Agrawal G P 2002 *J. Lightwave Technol.* **20** 790
Hirooka T and Wabnitz S 1999 *Electron. Lett.* **35** 655

[19] Li Q L and Li Q S 2006 *Chinese J. Laser* **33** 607 (in Chinese)

[20] Li Q L, Chen X D, Tang X H, Yuan X, Wang H and Lin L B 2004 *Chinese J. Laser* **31** 199 (in Chinese)

[21] Dinda P T, Nakkeeran K and Labruyere A 2002 *Opt. Lett.* **27** 382

[22] Anderson D 1983 *Phys. Rev.* A **27** 3135

[23] Akozbek N, Bowden C M and Talebpour A 2000 *Phys. Rev.* E **61** 4540